PrrC-anticodon nuclease: functional organization of a prototypical bacterial restriction RNase

Shani Blanga-Kanfi, Michal Amitsur, Abdussalam Azem and Gabriel Kaufmann*

Department of Biochemistry, Tel Aviv University, Ramat Aviv 69978, Israel

ABSTRACT

The tRNA^{Lys} anticodon nuclease PrrC is associated in latent form with the type Ic DNA restriction endonuclease EcoprrI and activated by a phage T4-encoded inhibitor of EcoprrI. The activation also requires the hydrolysis of GTP and presence of dTTP and is inhibited by ATP. The N-proximal NTPase domain of PrrC has been implicated in relaying the activating signal to a C-proximal anti-codon nuclease site by interacting with the requisite nucleotide cofactors [Amitsur *et al.* (2003) *Mol. Microbiol.,* 50, 129–143]. Means described here to bypass PrrC's self-limiting translation and thermal instability allowed purifying an active mutant form of the protein, demonstrating its oligomeric struc-ture and confirming its anticipated interactions with the nucleotide cofactors of the activation reaction. Mutagenesis and chemical rescue data shown impli-cate the C-proximal Arg^{320}, Glu^{324} and, possibly, His^{356} in anticodon nuclease catalysis. This triad exists in all the known PrrC homologs but only some of them feature residues needed for tRNA^{Lys} recognition by the *Escherichia coli* prototype. The differential conservation and consistent genetic linkage of the PrrC proteins with EcoprrI homologs portray them as a family of restriction RNases of diverse substrate specificities that are mobilized when an associated DNA restriction nuclease is compromised.

INTRODUCTION

Bacteria activate suicide programs in dire situations (1) including phage infection (2). A case in point is the tRNA^{Lys} anticodon nuclease (ACNase) PrrC (3–6) encoded by the optional *Escherichia coli prr* locus (7). ACNase activity is silenced by physical association of PrrC with the genetically linked type Ic DNA restriction endonuclease EcoprrI (8–11).

A phage T4-encoded peptide inhibitor of EcoprrI termed Stp activates the latent ACNase, possibly by altering the PrrC-EcoprrI interaction (10,12–18). The resultant transesterifying cleavage of tRNA^{Lys} (4) could block T4 late translation and contain the infection (19) but the T4-coded 3′-phosphatase/5′-polynucleotide kinase (Pnk) and RNA ligase1 (Rli1) normally offset the damage (4,20). PrrC homologs appear sporadically among distantly related bacteria always linked to EcoprrI homologs (17,18) (Figure 1).

High level expression of PrrC elicits overt (core) ACNase activity in *E.coli* (8,21) or cultured human cells (22) but self-limiting translation and thermal instability have impeded the isolation of the core ACNase protein in active form (21,23). Notions about the functional organization of PrrC have been inferred from sequence comparisons, mutagenesis and func-tional assays performed *in vivo* or with crude fractions. These data suggest that PrrC's N-proximal 2/3 harbors an ABC transporter-like NTPase (Figure 1) that mediates the acti-vation of ACNase by hydrolyzing GTP. Another co-activating nucleotide is dTTP that seems to cooperate with GTP without being hydrolyzed and effectively protects the core ACNase activity of free PrrC. ATP is yet another, negative effector of ACNase reaction. However, it has been uncertain whether all three nucleotides exert their effects through PrrC (18).

PrrC's remaining part contains residues involved in tRNA^{Lys} recognition (23–25). The main cues recognized in tRNA^{Lys} by PrrC are in the anticodon stem–loop region and comprise the anticodon bases, base modifications and base-pairing interactions (22–25). The transesterifying cleavage of tRNA^{Lys} catalyzed by PrrC resembles the first step in 'clas-sical' RNase reactions (26,27) where an entering 2′-oxygen displaces a leaving 5′ group at the phosphorous atom in a concerted in-line mechanism involving a pentameric transi-tion state phosphate (TSP). The classical RNases employ Glu or His as the general base, His as a general acid and Arg or Lys to neutralize the negative charge that develops on the TSP (28). Each of the three catalytic groups could provide upto 10^4-fold rate enhancement (29). Whether PrrC contains a similar catalytic triad has been unknown.

Means described here to bypass PrrC's self-limiting translation and thermal instability enabled (i) the isolation of an active mutant form of the core ACNase protein,

*To whom correspondence should be addressed. Tel: 972 3 642 6213; Fax: 972 3 640 6834; Email: gabika@tauex.tau.ac.il

The authors wish it to be known that, in their opinion, the first two authors should be regarded as joint First Authors.

Figure 1. Domain organization and sequence conservation of *E.coli* PrrC. The degree of conservation across the sequence of *E.coli* PrrC was processed and color-coded by ConSeq (Pupko *et al.* 2002; http://conseq.bioinfo.tau.ac.il) based on a ClustalW alignment (45) of the query sequence with sequences of 19 homologs. These homologs are encoded by the following bacteria and indicated by the respective accession numbers and three letter abbreviations: *Acidothiobacillus ferrooxidans* (Afe), nl|TIGR_920|contig:10033:a_ferrooxidans; *Actinobacillus pleuropneumoniae* (Apl), gnl|OUACGT_ 44294|ap5.fasta.screen.Contig198; *Azoarcus* sp. EbN1 (Azo), NC_006513.1; *Brevibacterium linens BL2* H (Bli), NZ_AAGP01000001.1|; *Burkholderia pseudomallei 1655* (Bup), NZ_AAHR01000011.1; *Haemophilus influenzae R2846* (Hin), ZP_00154666.1; *Leptospira interrogans* serovar Copenhageni str.(Lin), YP_000904.1; *Magnetococcus* sp. MC-1 (Mag), ZP_00289847.1: *Methylobacillus flagellatus* KT (Mfl), ZP_00201874.1;*Neisseria meningitidis MC58* (Nme), NP_273873.1*; Photorhabdus luminescens subsp. laumondii TTO1* (Plu), NP_931496.1; *Prosthecochloris aestuarii* DSM 271 (Pae), EAN22302.1; *Rhodopseudomonas palustris HaA2* (Rhp), NZ_AALQ01000003.1; *Shewanella baltica* OS155 (Sba), AAIO01000005.1; *Streptococcus equi* (Seq), gnl|Sanger_1336| Contig227; *Streptococcus mutans* (Smu), NC_004350.1; *Vibrio vulnificus* YJ016 (Vvu), NP_933608.1; *Xanthomonas campestris (*Xca), NC_003902.1. *Yersinia frederiksenii* ATCC 33641 (Yfr), ZP_00829622.1; Motifs and functional sites indicated over the sequence include those typical of ABC transporter ATPases (41) including the Walker A and B motifs, the ABC signature motif and the switch region or linchpin His (37); the 284–294 stretch implicated in recognition of the tRNA^{Lys} anticodon (23–25) and the putative ACNase catalytic triad Arg^{320}, Glu^{324} and His^{356} (this work). Conservation scale:

| 1 | 2 | 3 | 4 | 5 | 6 | 7 | 8 | 9 |

X-Insufficient data—the calculation for this site was performed on <10% of the sequences.

Variable   Average   Conserved

(ii) demonstrating its oligomeric, possibly tetrameric structure and (iii) confirming the anticipated interactions of PrrC with the nucleotides implicated in ACNase latency and activation. Other data suggest that the conserved Glu^{324}, Arg^{320} and, possibly, His^{356} partake in ACNase catalysis. This triad is conserved by all known PrrC homologs unlike the residues needed for tRNA^{Lys} recognition, suggesting that the PrrC proteins constitute a family of restriction RNases that vary in substrate specificity.

MATERIALS AND METHODS

Materials

The gel filtration calibration kit of native proteins was purchased from Pharmacia Biotech. Pre-stained Broad-Range and SeeBlue Plus 2 markers for calibrating polypeptide size in SDS–PAGE were purchased from New England Biolabs

or Invitrogen, respectively, TALON® immobilized-metal affinity resin from Clontech. The sources of other materials have been described (18,23,25).

PrrC mutants

The D222E mutant has been described (23). Missense mutants generated in this work were obtained by the Quick Change method (30). The His$_6$-tag was fused to PrrC's C-end by introducing first an Age I site that entailed an Asn^{394}→Thr replacement. This site served to insert a DNA fragment encoding a flexible linker, factor Xa site and His$_6$ [G$_3$S(G$_4$S)$_2$IEGRGSH$_6$]. The resultant fusion protein retained the parental ACNase activity and stability.

PrrC-expression plasmids and bacterial hosts

The PrrC proteins were expressed under the control of the T7-Lac promoter and Shine–Dalgarno sequence of plasmid

pRRC11 (23) in *E.coli* Rosetta (DE3)pLysS encoding rare tRNAs from plasmid pRARE (Novagen, UK) (31). The isogenic BL21:pLysS strain lacking pRARE was a control. PrrC protein was monitored by immunoblotting using purified polyclonal anti-PrrC antibodies (23).

ACNase assays

In vivo core ACNase activity was assayed by 5′ end-labeling the cleavage termini generated by ACNase using [γ-^{32}P]ATP and T4 Pnk, as described previously (18,23,24). Briefly, the labeling was performed on total low weight RNA extracted from cells induced to express the indicated form of PrrC and the products separated by denaturing gel electrophoresis along with controls from cells not expressing PrrC. The identity of the product has been ascertained by their migration with tRNA^{Lys} fragment 34–76, hybridization to complementary DNA probes and 5′ end-group analysis (18,23,24). The detection limit of this assay was estimated by serial dilutions of the RNA from the PrrC-expressing cells with RNA from isogenic, non-expressing cells. PrrC induction was limited to 30–45 min, during which ACNase products continue to accumulate also with wild-type PrrC. In the *in vitro* ACNase assays purified *E.coli* tRNA^{Lys} labeled with ^{32}P at the 33p34 cleavage junction was used as substrate (16). The standard reaction mixtures (10 μl) contained the indicated amount of PrrC [diluted where needed in buffer VI (detailed below) containing 1 mg/ml BSA], 1 fmol of the ^{32}P-labeled substrate (3000 Ci/mmol), 2 μM dTTP, 5 mM Na-HEPES buffer (pH 7.5); 0.5 mM MgCl$_2$, 15 mM NaCl, 5% glycerol and typically 0.25–0.5 M trimethylamine-N-oxide (TMAO). The reaction was performed at 10°C and terminated by adding 1.5 vol of 10 M urea, 0.01% bromphenol blue and 0.01% xylene cyanol. The products were separated by polyacrylamide–urea gel electrophoresis (18).

Bacterial growth and isolation of PrrC

E.coli Rosetta (DE3)pLysS transformants encoding the various PrrC forms were grown to ∼0.5 OD$_{600}$ at 37°C in Luria–Bertani (LB) medium containing 100 μg/ml ampicilin and 34 μg/ml chloramphenicol. A total of 1 mM isopropyl-β-D-thiogalactopyranoside (IPTG) was added to induce expression. The culture was shifted to 30°C and incubated for 2 h. All subsequent steps were at 0–4°C. The cells were harvested by centrifugation and the pellet washed twice in buffer I [10 mM Tris–HCl (pH 7.5); 15 mM MgCl$_2$, 1 M KCl and 10% glycerol], once in buffer II (Buffer I with 50 mM KCl) and then suspended at 1:1.5 w/v in buffer III [10 mM Na-HEPES (pH 7.5); 1 mM MgCl$_2$, 30 mM NaCl, Protease inhibitor cocktail tablet, EDTA-free (Roche); and 10% glycerol]. The cells were disrupted in an Amicon pressure cell at 18 000 psi and the lysate made upto 1–2 M TMAO and centrifuged for 30 min at 30 000 g in a Sorvall SS-34 rotor. The supernatant containing ∼30 mg/ml protein was supplemented with 2–10 μM dTTP and 5 mM imidazole and loaded at a 4:1 v/v ratio on a TALON column equilibrated with buffer IV (buffer III containing 10 μM dTTP, 5 mM imidazole and 2 M TMAO). The column was washed with 10 vol of the same buffer and the bound protein eluted with buffer V (buffer IV with 0.5 M imidazole). The eluted fraction was desalted by passage through a 2 ml Sephadex G-50 column

equilibrated with buffer VI (buffer III containing 2 μM dTTP, 1 M TMAO), loaded onto a 30 ml Superdex-200 XK16 gel filtration column (Pharmacia, separation range: $10^4 - 6 \times 10^5$ Da) equilibrated with buffer VI and fractionated in the Biologic HR chromatography system (Bio-Rad) at a flow rate of 0.25 ml/min. PrrC protein was monitored throughout the purification by protein staining, immunoblotting and core ACNase assay. The identity and purity of the PrrC protein band was ascertained by mass spectrometry.

Glutaraldehyde protein–protein crosslinking

The reaction was initiated by adding 0.01% glutaraldehyde to the indicated PrrC fraction kept at 0°C and terminated at the indicated time by adjusting the mixture to 0.1 M Tris–HCl buffer (pH 7.5). Samples were mixed with gel loading buffer, heated for 5 min at 100°C and separated on 10% or 5–13% gradient SDS–PAGE. The products were detected by staining with SeeBand Forte (GeBa) or immunoblotting.

UV-crosslinking nucleotides to PrrC

The UV-crosslinking mixture (10 μl) contained PrrC (post-TALON fraction in buffer III containing 1 M TMAO) at 50 ng with dTTP, 500 ng with GTP or ATP and the indicated concentrations of one of the following radio-labeled nucleotides: 0.2–5 μM [α-^{32}P]dTTP (300Ci/mmol) or 0.1–1.5 mM [α-^{32}P]GTP or ATP (1 Ci/mmol). The samples were placed in Cell-cut 60-well plates and irradiated from above at a distance of 10 cm for 5 min with a UV$_{254}$ lamp (UVGL-25, San Gabriel). The photolabeled product and total PrrC were separated by SDS–PAGE, transferred to a nitrocellulose membrane and visualized by autoradiography and immunoblotting.

Chemical rescue

Chemical rescue was measured by adding varying concentrations of guanidine, acetate, imidazole or phenol to ACNase reaction mixtures containing the indicated PrrC alleles. In calculating the rate enhancement nonspecific effects of the rescuing agent on the wild-type control were considered.

RESULTS

Isolation of the active oligomeric form of a PrrC mutant

Expression of PrrC inactivates essential tRNAs and inhibits translation, including PrrC's. However, PrrC mutants impaired in ACNase activity accumulate to higher levels, inversely proportional to the residual activity (23). This observation suggested that leaky PrrC mutants would facilitate the isolation of active core ACNase forms. One of them, PrrC-D222E, was chosen for further work due to its relatively high *in vitro* stability. Cells expressing PrrC-D222E featured lower *in vivo* ACNase activity than wild-type PrrC (23) (Figure 2A). Yet, the cell-free extract of the PrrC-D222E mutant was as active as the wild-type counterpart (Figure 2B). This difference was due to the higher *in vitro* stability of the mutant activity and, in turn, the higher level of the mutant protein. Namely, in the original cell extract the mutant activity decayed slower than the wild-type but similar decay rates were observed when the
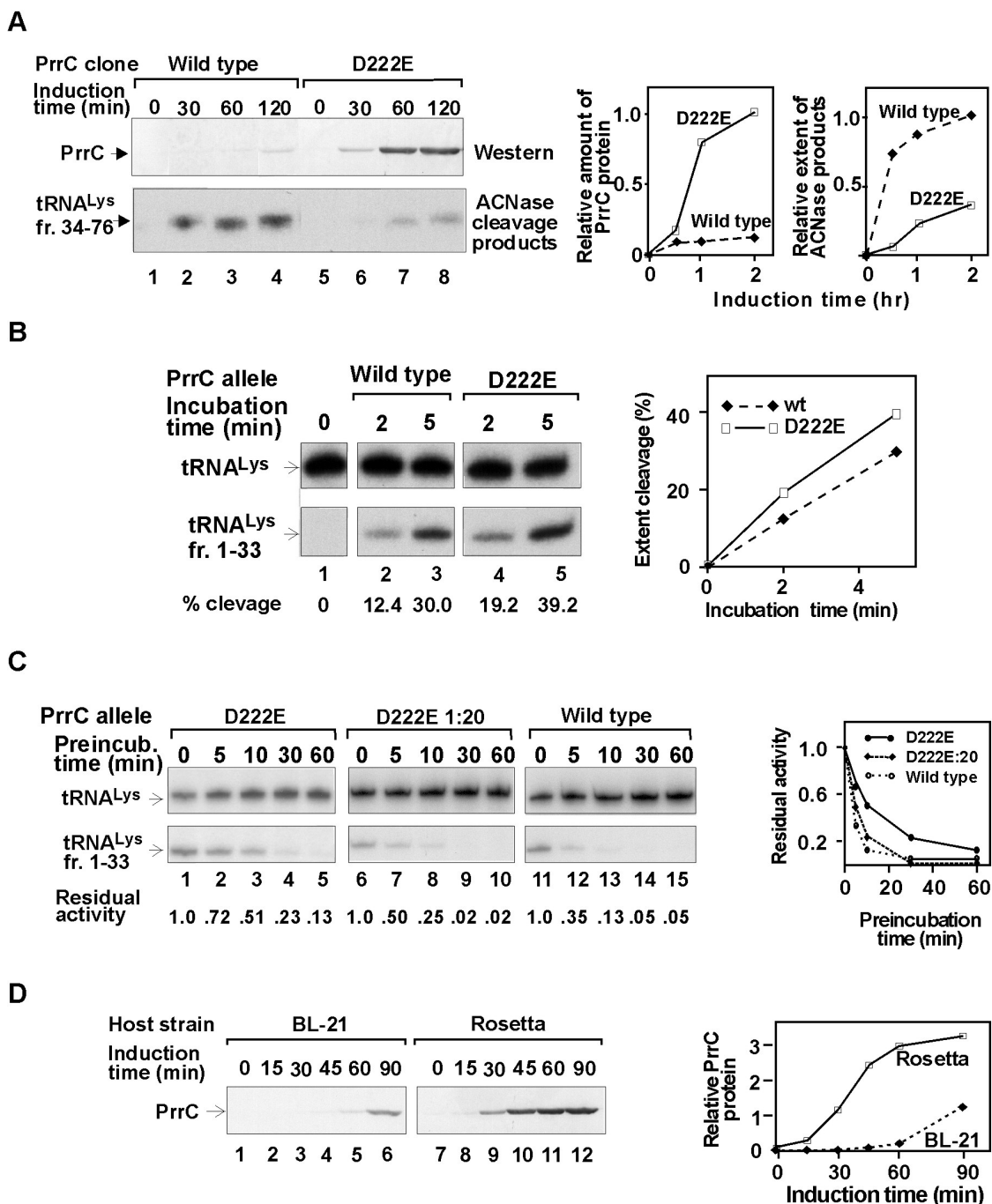
Figure 2. Protein levels and ACNase activities of wild-type and D222E alleles of PrrC. (**A**) *In vivo* levels of protein and ACNase cleavage products of the two PrrC forms. The expression of the two forms was induced by IPTG and the cellular levels of their protein and ACNase cleavage products were then determined as detailed in Materials and Methods. (**B**) *In vitro* ACNase activity of the indicated PrrC forms was determined as detailed in Materials and Methods. (**C**) Decay rates of the *in vitro* ACNase activity of wild-type and D222E forms of PrrC. The PrrC-D222E fraction was assayed as such or diluted 20-fold in an isogenic extract lacking PrrC. The dilution equalized the protein levels of the mutant and wild-type forms. Aliquots were pre-incubated at 37°C in the presence of 2 M TMAO and assayed for remaining ACNase activity at 10°C and 0.5 M TMAO under standard assay conditions. D222E 1:20 indicates D222E diluted 20-fold. (**D**) Levels of PrrC-D222E protein in the indicated *E.coli* strains.

concentrations of the two PrrC forms in the cell extract were equalized (Figure 2C). The PrrC protein yield could be further increased by expression in the Rosetta strain (Figure 2D), thus compensating for the abundant rare codons in *prrC*. However, co-expressing T4 Pnk and Rli1 to counteract ACNase cleavage increased the yield of wild-type PrrC

only (data not shown). Thus, the relatively weak activity of PrrC-D222E did not limit its translation.

ACNase activity could be further stabilized by the chemical chaperone TMAO that folds back denatured proteins and restores their enzymatic activities (32). This was shown by pre-incubating PrrC-D222E samples at 15–40°C with

0–2 M TMAO followed by assaying the remaining ACNase activity at 10°C and 1 M TMAO. The data indicated that the Tm of ACNase inactivation could increase upto ~10°C at 2 M TMAO (Figure 3). However, the presence of TMAO in the reaction mixture did not restore the activity once lost.

Core ACNase is stabilized also by dTTP (18), an effect added to that conferred by TMAO (data not shown). Therefore, both compounds were included in the enzyme fractions and column buffers during attempted purification of the core ACNase protein. These measures enabled purifying an active PrrC-D222E derivative containing a C-terminal His$_6$-tag (Materials and Methods) through immobilized-metal

affinity-chromatography and gel filtration (Figure 4A and B; Table 1). Wild-type PrrC was purified similarly but was rapidly inactivated (data not shown). For convenience, the His$_6$ derivative of PrrC-D222E is referred to below mostly as PrrC.

ACNase activity and PrrC protein eluted from the gel filtration column in peaks that almost completely overlapped and corresponded in position to a globular protein of ~200 kDa (Figure 4B). This suggested that the activity resides in a PrrC oligomer. Since the thermal inactivation of ACNase occurs without dissociation of the PrrC oligomer (Figure 5B), the subtle differences between the positions of PrrC and ACNase peaks could reflect the different shapes of active and inactive PrrC forms rather than size heterogeneity. Glutaraldehyde protein–protein crosslinking performed on the post-TALON or the gel filtration fractions yielded three groups of product bands migrating in SDS–PAGE slower than the PrrC monomer (shown in Figure 4C for the post-TALON fraction). Judged from the position of these products relative to the size markers they were considered as different crosslinking versions of dimer, trimer and tetramer forms. Such a pattern with a relatively low level of trimer bands has been observed with known dimer of dimers proteins, including an ABC transporter ATPase (33–36).
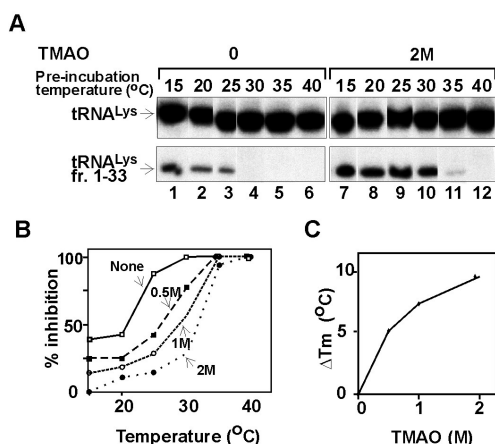

Figure 3. TMAO stabilizes ACNase activity. (**A**) PrrC-D222E aliquots were pre-incubated at the indicated temperatures for 30 min without or with 2 M TMAO. ACNase activity was assayed then for 20 min at 10°C with 1 M TMAO. (**B**) Inhibition of ACNase activity as a function of pre-incubation temperature and TMAO level. (**C**) Tm of ACNase inactivation versus TMAO level.

Table 1. PrrC-core ACNase purification

Step	Protein (mg)	ACNase (units[a])	Specific activity (U/mg)	Yield	Purification
S-30	20	16 000	800	100	1
TALON	0.3	9500	32	59	39
Superdex-200	0.18	6000	33	37	41

[a] One ACNase unit is defined as 1 fmol tRNA^{Lys} cleaved per min at 10°C under standard assay conditions (Materials and Methods).
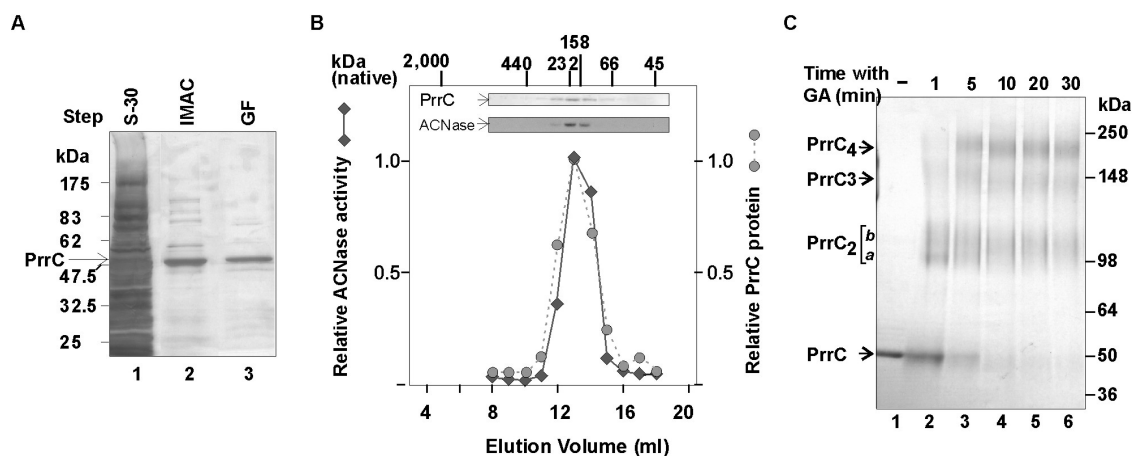

Figure 4. Isolation of PrrC and determination of its oligomeric structure. (**A**) PrrC-D222E-His6 was purified by high-speed centrifugation (S-30), immobilized cobalt affinity-chromatography (IMAC) and Superdex-200 gel filtration (GF) as detailed in Materials and Methods and Table 1. Aliquots of the indicated fractions were separated by SDS–PAGE and silver stained. (**B**) Superdex-200-elution profile of PrrC protein and ACNase activity. The TALON fraction of PrrC was fractionated on a Superdex-200 column. ACNase activity and PrrC protein were detected in the eluted fractions as described in Materials and Methods. The top inset shows the profile of SeeBlue stained PrrC protein, the lower inset the profile of the ACNase cleavage product of tRNA^{Lys} kDa—native protein size markers. (**C**) GA-crosslinking profile of PrrC. The post-TALON fraction of PrrC was subjected to glutaraldehyde crosslinking. Aliquots taken at the indicated times were separated by 5–13% gradient SDS–PAGE and visualized by staining, as detailed in Materials and Methods. kDa—protein size markers. PrrC$_{2, 3 \& 4}$ indicate putative PrrC dimer, trimer and tetramer forms, respectively.
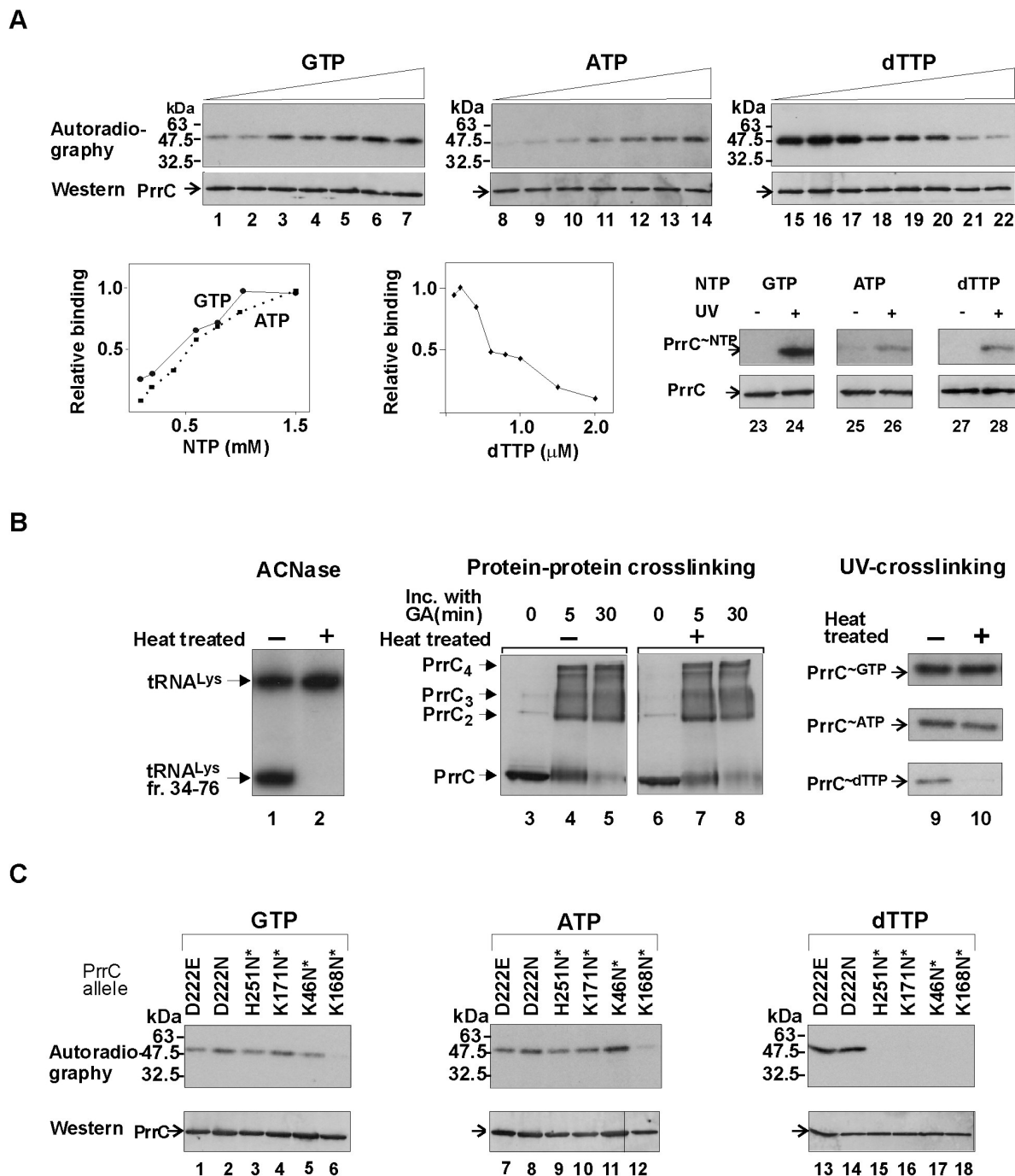
Figure 5. UV-crosslinking nucleotides to PrrC. (**A**) PrrC was incubated with the indicated concentrations of radio-labeled GTP (lanes 1–7, 0.1, 0.2, 0.4, 0.6, 0.8, 1.0 and 1.5 mM, respectively), ATP (lanes 8–14, 0.1, 0.2, 0.4, 0.6, 0.8, 1.0 and 1.5 mM, respectively) or dTTP (lanes 15–22, 0.1, 0.2, 0.4, 0.6, 0.8, 1.0, 1.5 and 2.0 μM, respectively) and UV-irradiated. The controls with and without radiation contained 0.5 mM GTP (lanes 23 and 24), 0.5 mM ATP (lanes 25 and 26) or 0.2 μM dTTP (lanes 27 and 28). The samples were separated by 10% SDS–PAGE, transferred to a nitrocellulose membrane, autoradiographed and immunoblotted (Materials and Methods). (**B**) Effect of heat inactivation of ACNase on PrrC's ability to UV-crosslink nucleotides and oligomeric structure. Untreated PrrC or heat inactivated aliquots (2 min at 40°C) were assayed for ACNase activity (lanes 1 and 2), glutaraldehyde protein–protein crosslinking (lanes 3–8) and UV-crosslinking the indicated nucleotides (lanes 9 and 10). (**C**) The indicated PrrC alleles were assayed for ability to UV-crosslink GTP (lanes 1–6), ATP (lanes 7–12) or dTTP (lanes 13–18). The asterisk in the K46N*, K168N*, K171N* and H251N* labels indicate that these mutations were introduced over the D222E background.

Nucleotide binding attributes of PrrC

PrrC's interaction with nucleotides affecting ACNase activation was investigated by UV-crosslinking. GTP, ATP and dTTP yielded each a conjugate that coincided in SDS–PAGE with monomeric PrrC (Figure 5A). Such products were absent from or severely decreased in the non-irradiated controls (lanes 23–28). The conjugates formed with GTP or with ATP featured sigmoidal dose-response

patterns with EC_{50} of ~0.5 mM (lanes 1–7 and 8–14, respectively). In contrast, the dTTP conjugate peaked at ~0.2 μM and declined above this level (lanes 15–22). This was unexpected since dTTP stabilizes core ACNase in a sigmoidal dose-response pattern and its protective effect does not level off even at 10 μM (18).

Inactivating ACNase by heating it for 2 min at 40°C (Figure 5B, lanes 1 and 2) did not significantly affect the oligomeric organization (lanes 3–8) or ability to UV-crosslink GTP or ATP, but abolished the UV-crosslinking to dTTP (lanes 9 and 10).

Next we investigated the effects of NTPase motif mutations introduced over the D222E background on the ability of the three nucleotides to UV-crosslink PrrC. Mutating K46 (Walker A), K171 (ABC signature) or H251 [corresponding to the linchpin His of ABC-transporter ATPases, Ref. (37)] had no apparent effect on the interactions of PrrC with GTP (Figure 5C, lanes 3–5) or ATP (lanes 9–11) but nearly abolished the interaction with dTTP (lanes 15–17). However, mutating the conserved K168 found immediately upstream to the ABC signature motif severely inhibited the UV-crosslinking of all three nucleotides (lanes 6, 12 and 18). All the double mutants investigated lacked ACNase activity but were soluble and retained the typical oligomeric structure (data not shown). The single D222E and D222N mutants had similar ACNase activities and protein levels (data not shown) and interacted similarly with each of the three nucleotides (lanes 1, 2, 7, 8, 13 and 14).

Mutagenesis of potentially functional C-domain residues

A catalytic ACNase site was looked for by mutating conserved and potentially functional C-domain residues using the conserved N-domain His[251] and less conserved C-domain residues as controls. The mutations were introduced over the wild-type background and their effects on the *in vivo* core ACNase activity and level of PrrC protein determined. Replacing the conserved Arg[320] by Ala or Gln reduced ACNase activity below detection and increased the protein yield 20- to 40-fold over wild-type (Figure 6, lanes 1–3). The isofunctional R320K mutant retained trace activity
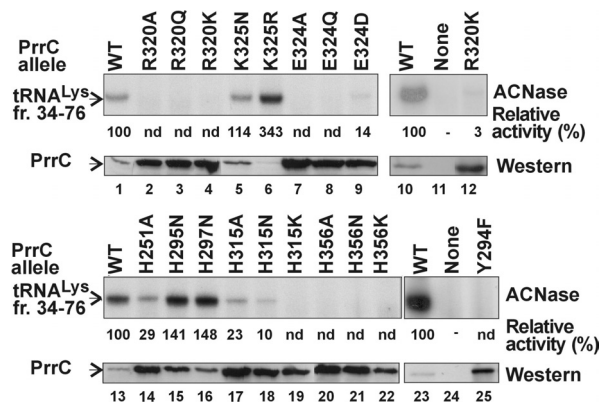
detected in some experiments (lanes 4, 10–12). In contrast, Lys[325] that is present in 18/20 PrrC homologs (Figure 8) seemed nonessential. Replacing it with Asn (Figure 6, lane 5) or Ala (data not shown) had no effect on the activity and the K325R mutation even stimulated it 2- to 3-fold. The latter mutation reduced the PrrC protein level considerably (compare lanes 1 and 6), possibly due to stronger inhibition of translation. Replacing the conserved Glu[324] (Figures 1 and 8) by Gln or Ala reduced the activity below detection and enhanced the protein level (Figure 6, lanes 7 and 8) but the isofunctional E324D mutation was less inhibitory (lane 9). The non-conserved Asp[341] and Glu[371] could be replaced without apparent loss of activity (data not shown). Each of the three His[356] missense mutants investigated lacked detectable ACNase activity whereas His[315] or His[251] mutants featured over 20% the wild-type extent of cleavage. Mutating His[295] had virtually no effect (Figure 6, lanes 13–18 and 20–22). Finally, replacing Tyr[294] with Phe (Figure 6, lanes 23–25) or Ser (data not shown) inactivated ACNase. Tyr[294] was also probed because equivalents of this residue exist in a large subset of the known PrrC proteins and the remaining homologs contain His instead (Figure 8). Moreover, a Tyr residue could partake in the active site of an archaeal tRNA splicing endonuclease (38).

Chemical rescue of suspected ACNase site mutants

The possible contributions of Arg[320], Glu[324], His[356] and Tyr[294] to ACNase catalysis were further investigated by attempted chemical rescue of their respective to-alanine or to-serine mutants. In this approach a missing functional side chain is substituted by a corresponding small molecule. Partial restoration of the activity suggests that the mutant retained the functional conformation and failed to act because it lacked the critical side chain (39). As shown, guanidine activated R320A (Figure 7A, lanes 1–6) but not E324A (lanes 7–12) and ammonium acetate rescued E324A (Figure 7B, lanes 13–18) but not R320A (lanes 19–24). Sodium and ammonium acetate acted similarly (data not shown), indicating that the rescuing agent was acetate. However, H356A was not rescued by imidazole or its 2- or 4-methyl derivatives. Y294S was not rescued by phenol, imidazole or acetate (data not shown). The rescue of Y294 was attempted also with the latter two agents due to replacement of Tyr[294] by His in some PrrC homologs and because the Y142S mutant of porcine isocitrate dehydrogenase is rescued by acetate (40).

Figure 6. *In vivo* ACNase activity and protein level of PrrC mutants. The indicated PrrC mutants were compared to the wild-type allele *in vivo* ACNase activity by radiolabeling the resultant 5′-OH cleavage termini and for PrrC protein level by western blotting as detailed in Materials and Methods.

DISCUSSION

Functional segregation of PrrC's nucleotide binding sites (NBS)

The glutaraldehyde crosslinking pattern of PrrC (Figure 4C) resembles those of known dimer of dimers proteins, including an ABC-transporter ATPase (33–36). Therefore, PrrC could be similarly organized. However, this assumption remains to be tested by more accurate size determinations and using further stabilized forms of PrrC amenable to such analyses.

NBS arise in ABC-transporter ATPases by coalescence of a Walker A motif of one subunit and ABC signature motif
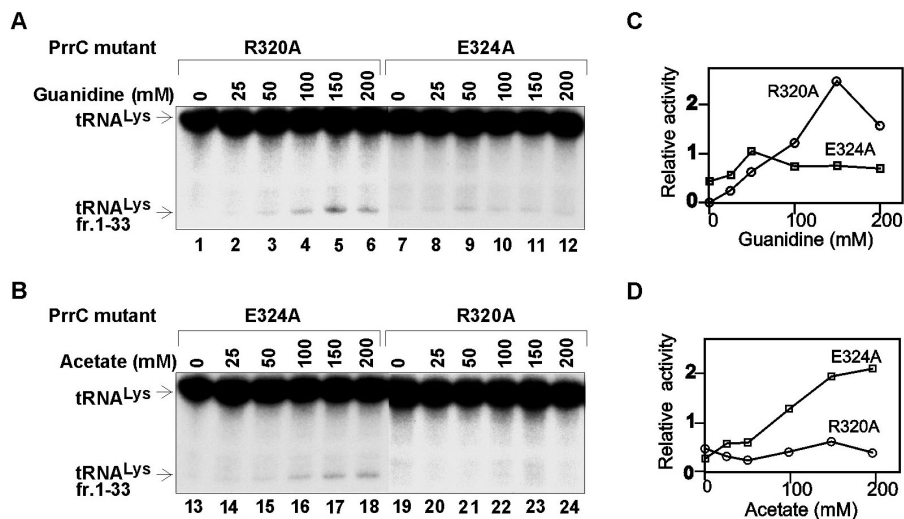
Figure 7. Chemical rescue of PrrC mutants. (**A**) The indicated PrrC alleles were assayed for ACNase activity in the presence of the indicated concentrations of guanidine-HCl or (**B**) ammonium acetate. (**C**) Relative ACNase activities versus guanidine-HCl or (**D**) ammonium acetate concentration.

of another within a head-to-tail dimer (41). Therefore, as a dimer of dimers, PrrC could contain four such NBS. However, these NBS could segregate into distinct subtypes specific for GTP or dTTP, as indicated by the following facts. First, the dose-response patterns the two nucleotides featured in their UV-crosslinking to PrrC (Figure 5A) confirmed the vastly higher affinity of dTTP for the protein, previously inferred from the patterns of core ACNase protection by dTTP and the GTP requirement in ACNase activation (18). Second, GTP featured in the UV-crosslinking to PrrC the anticipated sigmoidal-like dose-response whereas dTTP yielded an unexpected optimum pattern (Figure 5A). Third, changes in PrrC that entailed loss of ACNase activity without disruption of the oligomeric structure of the protein, induced by mild heating (Figure 5B) or mutating conserved NTPase positions (Figure 5C), also abolished the UV-crosslinking of PrrC to dTTP but not to GTP (Figure 5B). Fourth, GTP and dTTP have been shown to cooperate in ACNase activation but only GTP seemed to be hydrolyzed in the process (18). Taken together, these facts reinforce the notion that PrrC contains a subset of low-affinity, catalytic NBS specific for GTP and a high-affinity subset specific for dTTP. Since both types are likely determined by the same NTPase motifs, their distinguishing features could be acquired by asymmetric subunit packing.

As mentioned, dTTP UV-crosslinked PrrC optimally at a sub-µM level but poorly at higher levels where it effectively protected the core ACNase activity (18). This discrepancy may be reconciled by suggesting that during the cooperative binding of dTTP to PrrC the protein undergoes a structural change that shifts the photoreactive amino acid away from the nucleotide base. The sensitivity of the PrrC-dTTP interaction to modest changes in PrrC's structure was also indicated by the observations that mild heat treatment (Figure 5B) or certain NTPase mutations (Figure 5C) abolished the UV-crosslinking of PrrC to dTTP but not to GTP.

The similar dose-response patterns GTP exhibited in UV-crosslinking PrrC (Figure 5A) or ACNase activation (18) suggest that PrrC harbors the activating GTPase, although such

an activity remains to be demonstrated. It is noteworthy that Asp^{222} of PrrC's Walker B motif could be important for hydrolysis of the bound nucleotide as in well-characterized ATPases (42). Thus, the Asp^{222} mutants used here could be devoid of the anticipated GTPase activity.

GTP and ATP were similarly UV-crosslinked to PrrC (Figure 5A). Therefore, they could exert their opposing effects in ACNase activation by competing over the same low-affinity NBS. Presumably, ATP binding to PrrC within the ACNase holoenzyme safeguards the latent state and replacing it with GTP could alleviate this inhibition.

Is dTTP an obligatory co-activator of ACNase?

Latent ACNase can be activated *in vitro* without Stp by adding dTTP, albeit, at levels far higher than needed to protect core ACNase (18) or UV-crosslink PrrC (Figure 5A). This alternative mode of activation could be taken to indicate that ACNase is mobilized also in cellular stress situations other than T4 infection. Alternatively, dTTP is an obligatory co-activator of ACNase rendered more accessible to PrrC within the latent holoenzyme by the T4-encoded peptide. According to the latter interpretation, the excessive amount of dTTP that enabled activating ACNase in the absence of Stp helped bypass the requirement for Stp. Likewise, the small amounts of dTTP in the cell-free extract sufficed for activating ACNase when Stp was present. Further credence to the notion that dTTP is an obligatory co-activator and ACNase is mobilized specifically during phage T4 infection is lent by (i) the increase in the cellular level of dTTP before the onset of T4 DNA replication and ACNase activation (18,43) and (ii) the sporadic distribution of PrrC among bacteria (Figure 1), indicative of a niche-function rather than participation in a general stress response.

The ACNase site

The *in vivo* ACNase assay allowed us to detect ~10^2-fold reduction in the extent of tRNA cleavage products considered here an indirect measure of the reaction rate. However, the
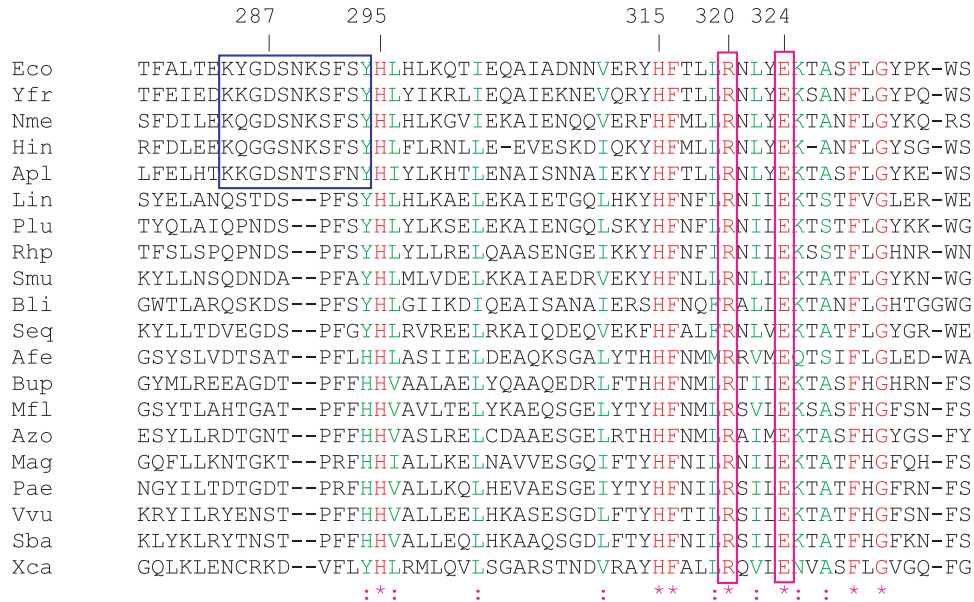
Figure 8. PrrC residues implicated in tRNA[Lys] recognition and cleavage. The multiple sequence alignment was derived as in the legend to Figure 1. The portion shown corresponds to residues 278–335 of the *E.coli* query. Residues marked in red are identical, in green similar. The blue box indicates consensus sequence implicated in tRNA[Lys] recognition. The magenta box marks residues implicated in ACNase catalysis.

actual value could be closer to the 10^{3-4}-fold rate reduction expected from loss of a catalytic RNase group (44) because the mutant proteins were more abundant than wild-type PrrC (Figure 6). This consideration, taken with (i) the conservation of Arg[320] and Glu[324], (ii) the null phenotypes of the isosteric and alanine mutants of Arg[320] and Glu[324], (iii) the leaky phenotypes of their isofunctional mutants (Figure 6) and (iv) the chemical rescue data (Figure 7) strongly suggest that Arg[320] and Glu[324] partake in ACNase catalysis. Specifically, the positively charged Arg[320] could be the TSP stabilizer and Glu[324] the general base catalyst, by analogy with classical RNases that delegate this function to Glu or His. In contrast, the general acid catalyst is always a His residue (28). His[356] seems the best candidate for the latter function by default, due to its conservation and, importantly, the failure of its missense mutants to elicit detectable ACNase activity (Figure 6). In contrast, mutating other conserved His residues had milder or no effect on ACNase activity. Nonetheless, the failure to chemically rescue the H356A mutant calls for further examination of the His[356] assignment. Tyr[294] also seems a less likely candidate for a catalytic role despite the null phenotypes of its mutants. Namely, this residue is only partially conserved among the PrrC homologs. Moreover, as indicated below, it could partake in tRNA[Lys] binding. The putative Arg[320]-Glu[324]-His[356] ACNase triad resembles in composition that of RNase T1 (26) and, hence, could assume a similar arrangement about the substrate's scissile phosphodiester linkage. However, in view of the oligomeric structure of PrrC the possibility that the ACNase site is shared by interfacing subunits should also be considered.

The PrrC restriction RNases

As mentioned, all known PrrC proteins feature the Arg[320]-Glu[324]-His[356] triad (Figure 8). Therefore, they are also expected to function all as RNases. Moreover, all of them feature the N-proximal NTPase motifs (Figure 1) and are genetically linked to EcoprrI homologs. Hence, they could all function as second-strike restriction RNases, i.e. being activated to counteract phage infection when the associated DNA restriction nuclease is compromised by the phage, as with the *E.coli* prototype (17). Another shared motif, rich in acidic, hydrophobic and aromatic residues ('PrrC box', residues 68–94 in Figure 1) is unique to the PrrC family. Hence, it likely plays a specific role, e.g. interfacing EcoprrI and/or communicating with the ACNase domain.

Residues Asp[287] and Ser[288] of *E.coli* PrrC have been implicated in tRNA[Lys] recognition (23–25). Preliminary peptide mimicry data suggest that a contiguous stretch to which these residues belong interacts with the tRNA[Lys] anticodon (D. Klaiman, S. Blanga, M. Amitsur and G. Kaufmann; unpublished data). This stretch includes the essential aromatic residues Phe[292] (23) and Tyr[294] (Figure 6) and coincides with a consensus sequence shared by a subset of PrrC homologs more closely related to the *E.coli* prototype than the other homologs (Figure 8). In the remaining homologs the corresponding region differs considerably in sequence. Therefore, these homologs likely target one or more different RNA structures.

Clearly, functional characterization of the PrrC homologs will be required to examine these various expectations, which rest mainly on DNA sequence data.

REFERENCES

1. Yarmolinsky,M.B. (1995) Programmed cell death in bacterial populations [comment]. *Science*, **267**, 836–837.
2. Snyder,L. (1995) Phage-exclusion enzymes: a bonanza of biochemical and cell biology reagents? *Mol. Microbiol.*, **15**, 415–420.
3. David,M., Borasio,G.D. and Kaufmann,G. (1982) Bacteriophage T4-induced anticodon-loop nuclease detected in a host strain restrictive to RNA ligase mutants. *Proc. Natl Acad. Sci. USA.*, **79**, 7097–7101.
4. Amitsur,M., Levitz,R. and Kaufmann,G. (1987) Bacteriophage T4 anticodon nuclease, polynucleotide kinase and RNA ligase reprocess the host lysine tRNA. *EMBO J.*, **6**, 2499–2503.
5. Snyder,L. and Kaufmann,G. (1994) T4 phage exclusion mechanisms. In Karam,J.D., Drake,J.W., Kreuzer,K.N., Mosig,G., Hall,D.W., Eiserling,F.A., Black,L.W., Spicer,E.K., Kutter,E., Carlson,K. and Miller,E.S. (eds), *Molecular Biology of bacteriophage T4*. ASM Press, Washington, D.C., pp. 391–396.
6. Kaufmann,G. (2000) Anticodon nucleases. *Trends Biochem. Sci.*, **25**, 70–74.
7. Abdul-Jabbar,M. and Snyder,L. (1984) Genetic and physiological studies of an *Escherichia coli* locus that restricts polynucleotide kinase and RNA ligase mutants of bacteriophage T4. *J. Virol.*, **51**, 522–529.
8. Levitz,R., Chapman,D., Amitsur,M., Green,R., Snyder,L. and Kaufmann,G. (1990) The optional *E. coli prr* locus encodes a latent form of phage T4-induced anticodon nuclease. *EMBO J.*, **9**, 1383–1389.
9. Linder,P., Doelz,R., Gubler,M. and Bickle,T.A. (1990) An anticodon nuclease gene inserted into a *hsd* region encoding a type I DNA restriction system. *Nucleic Acids Res.*, **18**, 7170.
10. Amitsur,M., Morad,I., Chapman-Shimshoni,D. and Kaufmann,G. (1992) HSD restriction-modification proteins partake in latent anticodon nuclease. *EMBO J.*, **11**, 3129–3134.
11. Tyndall,C., Meister,J. and Bickle,T.A. (1994) The *Escherichia coli* prr region encodes a functional type IC DNA restriction system closely integrated with an anticodon nuclease gene. *J. Mol. Biol.*, **237**, 266–274.
12. Depew,R.E. and Cozzarelli,N.R. (1974) Genetics and physiology of bacteriophage T4 3'-phosphatase: evidence for the involvement of the enzyme in T4 DNA metabolism. *J. Virol.*, **13**, 888–897.
13. Runnels,J., Soltis,D., Hey,T. and Snyder,L. (1982) Genetic and physiological studies of the role of RNA ligase of bacteriophage T4. *J. Mol. Biol.*, **154**, 273–286.
14. Kaufmann,G., David,M., Borasio,G.D., Teichmann,A., Paz,A., Amitsur,M., Green,R. and Snyder,L. (1986) Phage and host genetic determinants of the specific anticodon-loop cleavages in bacteriophage T4 infected *Escherichia coli* CTr5X. *J. Mol. Biol.*, **188**, 15–22.
15. Chapman,D., Morad,I., Kaufmann,G., Gait,M.J., Jorissen,L. and Snyder,L. (1988) Nucleotide and deduced amino acid sequence of *stp*: the bacteriophage T4 anticodon nuclease gene. *J. Mol. Biol.*, **199**, 373–377.
16. Amitsur,M., Morad,I. and Kaufmann,G. (1989) *In vitro* reconstitution of anticodon nuclease from components encoded by phage T4 and *Escherichia coli* CTr5X. *EMBO J.*, **8**, 2411–2415.
17. Penner,M., Morad,I., Snyder,L. and Kaufmann,G. (1995) Phage T4-coded Stp: double-edged effector of coupled DNA and tRNA-restriction systems. *J. Mol. Biol.*, **249**, 857–868.
18. Amitsur,M., Benjamin,S., Rosner,R., Chapman-Shimshoni,D., Meidler,R., Blanga,S. and Kaufmann,G. (2003) Bacteriophage T4-encoded Stp can be replaced as activator of anticodon nuclease by a normal host cell metabolite. *Mol. Microbiol.*, **50**, 129–143.
19. Sirotkin,K., Cooley,W., Runnels,J. and Snyder,L. (1978) A role in true-late gene expression for the T4 bacteriophage 5'-polynucleotide kinase 3'-phosphatase. *J. Mol. Biol.*, **123**, 221–233.
20. Ho,C.K. and Shuman,S. (2002) Bacteriophage T4 RNA ligase 2 (gp24.1) exemplifies a family of RNA ligases found in all phylogenetic domains. *Proc. Natl Acad. Sci. USA.*, **99**, 12709–12714.
21. Morad,I., Chapman-Shimshoni,D., Amitsur,M. and Kaufmann,G. (1993) Functional expression and properties of the tRNA(Lys)-specific core anticodon nuclease encoded by *Escherichia coli* prrC. *J. Biol. Chem.*, **268**, 26842–26849.
22. Shterman,N., Elroy-Stein,O., Morad,I., Amitsur,M. and Kaufmann,G. (1995) Cleavage of the HIV replication primer tRNALys,3 in human cells expressing bacterial anticodon nuclease. *Nucleic Acids. Res.*, **23**, 1744–1749.
23. Meidler,R., Morad,I., Amitsur,M., Inokuchi,H. and Kaufmann,G. (1999) Detection of anticodon nuclease residues involved in tRNALys cleavage specificity. *J. Mol. Biol.*, **287**, 499–510.
24. Jiang,Y., Meidler,R., Amitsur,M. and Kaufmann,G. (2001) Specific interaction between anticodon nuclease and the tRNA(Lys) wobble base. *J. Mol. Biol.*, **305**, 377–388.
25. Jiang,Y., Blanga,S., Amitsur,M., Meidler,R., Krivosheyev,E., Sundaram,M., Bajji,A.C., Davis,D.R. and Kaufmann,G. (2002) Structural features of tRNALys favored by anticodon nuclease as inferred from reactivities of anticodon stem and loop substrate analogs. *J. Biol. Chem.*, **277**, 3836–3841.
26. Steyaert,J. (1997) A decade of protein engineering on ribonuclease T1—atomic dissection of the enzyme-substrate interactions. *Eur. J Biochem.*, **247**, 1–11.
27. Raines,R.T. (1998) Ribonuclease A. *Chem. Rev.*, **98**, 1045–1065.
28. Gerlt,J.A. (1993) Mechanistic principles of enzyme-catalyzed cleavage of phosphodiester bonds. In Linn,S.M., Lloyd,R.S. and Roberts,R.J. (eds), *Nucleases*. Cold Spring Harbor Laboratory Press, Plainview NY, Vol 25, pp. 1–34.
29. Emilsson,G.M., Nakamura,S., Roth,A. and Breaker,R.R. (2003) Ribozyme speed limits. *RNA*, **9**, 907–918.
30. Ansaldi,M., Lepelletier,M. and Mejean,V. (1996) Site-specific mutagenesis by using an accurate recombinant polymerase chain reaction method. *Anal. Biochem.*, **234**, 110–111.
31. Studier,F.W. (1991) Use of bacteriophage T7 lysozyme to improve an inducible T7 expression system. *J. Mol. Biol.*, **219**, 37–44.
32. Baskakov,I. and Bolen,D.W. (1998) Forcing thermodynamically unfolded proteins to fold. *J. Biol. Chem.*, **273**, 4831–4834.
33. Hajdu,J., Bartha,F. and Friedrich,P. (1976) Crosslinking with bifunctional reagents as a means for studying the symmetry of oligomeric proteins. *Eur. J. Biochem.*, **68**, 373–383.
34. Hucho,F., Mullner,H. and Sund,H. (1975) Investigation of the symmetry of oligomeric enzymes with bifunctional reagents. *Eur. J. Biochem.*, **59**, 79–87.
35. Azem,A., Weiss,C. and Goloubinoff,P. (1998) Structural analysis of GroE chaperonin complexes using chemical cross-linking. *Meth. Enzymol.*, **290**, 253–268.
36. Denis,M., Haidar,B., Marcil,M., Bouvier,M., Krimbou,L. and Genest,J. (2004) Characterization of oligomeric human ATP binding cassette transporter A1. Potential implications for determining the structure of nascent high density lipoprotein particles. *J. Biol. Chem.*, **279**, 41529–41536.
37. Zaitseva,J., Jenewein,S., Jumpertz,T., Holland,I.B. and Schmitt,L. (2005) H662 is the linchpin of ATP hydrolysis in the nucleotide-binding domain of the ABC transporter HlyB. *EMBO J.*, **24**, 1901–1910.
38. Li,H., Trotta,C.R. and Abelson,J. (1998) Crystal structure and evolution of a transfer RNA splicing enzyme. *Science*, **280**, 279–284.
39. Carter,P. and Wells,J.A. (1987) Engineering enzyme specificity by 'substrate-assisted catalysis'. *Science*, **237**, 394–399.
40. Kim,T.K., Lee,P. and Colman,R.F. (2003) Critical role of Lys212 and Tyr140 in porcine NADP-dependent isocitrate dehydrogenase. *J. Biol. Chem.*, **278**, 49323–49331.
41. Chen,J., Lu,G., Lin,J., Davidson,A.L. and Quiocho,F.A. (2003) A tweezers-like motion of the ATP-binding cassette dimer in an ABC transport cycle. *Mol. Cell*, **12**, 651–661.
42. Hu,C.Y., Chen,W. and Frasch,W.D. (1999) Metal ligation by Walker homology B aspartate betaD262 at site 3 of the latent but not activated form of the chloroplast F(1)-ATPase from *Chlamydomonas reinhardtii*. *J. Biol. Chem.*, **274**, 30481–30486.

43. Greenberg,G.R., He,P., Hilfinger,J. and Tseng,M.J. (1994) Deoxyribonucleoside triphosphate synthesis and phage T4 DNA replication. In Karam,J.D., Drake,J.W., Kreuzer,K.N., Mosig,G., Hall,D.W., Eiserling,F.A., Black,L.W., Spicer,E.K., Kutter,E., Carlson,K. and Miller,E.S. (eds), *Molecular Biology of Bacteriophage T4*. American Society for Microbiology, Washington D.C., pp. 14–27.

44. Breaker,R.R., Emilsson,G.M., Lazarev,D., Nakamura,S., Puskarz,I.J., Roth,A. and Sudarsan,N. (2003) A common speed limit for RNA-cleaving ribozymes and deoxyribozymes. *RNA*, **9**, 949–957.

45. Thompson,J.D., Higgins,D.G. and Gibson,T.J. (1994) CLUSTAL W: improving the sensitivity of progressive multiple sequence alignment through sequence weighting, position-specific gap penalties and weight matrix choice. *Nucleic Acids Res.*, **22**, 4673–4680.